

Attenuation Coefficients for Layered Ceiling and Floor Shields in PET/CT Clinics

Robert L. Metzger and Kenneth A. Van Riper

*Radiation Safety Engineering, Inc
3245 North Washington Street, Chandler, AZ 85225
rlmetzger@radsafe.com; kvr@rt66.com*

INTRODUCTION

Positron Emission Tomography (PET) is enjoying explosive growth due to its ability to accurately stage many types of cancer and follow the progress of treatments. The facilities present unique challenges in shielding design due to the nature of the study, and the desire to place the facilities near other imaging and treatment clinics.

A typical PET patient will receive 555 MBq (15 mCi) of ¹⁸F labeled 2-Fluoro-2-Deoxy-D-Glucose (¹⁸FDG) and will rest in a darkened room (called a quiet room) for 45 minutes to allow the drug to localize in the lesions of interest. A normal clinic will have one to three quiet rooms. While in the quiet room, the patient will normally recline in a comfortable lounge chair.

The distribution of the ¹⁸FDG in the patient will vary from patient to patient, but much of the isotope will be located in the brain and the bladder. After resting for approximately 45 minutes, the patient is asked to empty his or her bladder, and is placed on the scanner bed. Images are collected for 30 to 45 minutes on the PET or combined PET/CT unit. The patient is then released after the scanning is complete.

Shielding design for PET/CT clinics is frequently difficult as many of the facilities are being retrofitted into existing imaging centers and hospitals where space is cramped. The patient quiet rooms, the hot laboratory, and the scanners are commonly positioned in close proximity to uncontrolled areas where non-occupational dose limits apply. Of particular concern are the ceiling and floor shields for the quiet and the scanner rooms because these are constructed by adding sheets of lead to the existing concrete ceiling and floor decks. Much of the cost of shielding in a PET/CT clinic is driven by the installation costs of these shields. The attenuation provided by these layered shields is difficult to calculate by point kernel methods. An underestimation of the shielding effectiveness will result in additional lead and higher cost.

CLINIC ROOM MODELS

Wall shielding is constructed of commercial sheet lead and can easily be calculated using point kernel techniques^[1, 2] with appropriate buildup factors. When occupied areas exist above or below the PET clinic, however, the shielding is constructed of the existing concrete floor deck and commercial sheet lead applied to the top of the floor, or, more commonly, suspended from the floor joists. Concrete floor decks in medical office buildings typically range from 5 to 15 cm in thickness, while hospitals designed for heavy floor loading can exceed 20 cm in thickness. The concrete floor decks in existing

structures may be constructed of normal density concrete (2.35 g/cm³) or lightweight concrete, and the poured thickness may vary from the specified amount by 1 cm or more.

The layered lead and concrete shield is difficult to estimate by point kernel techniques as the energy of the photons incident on each layer is difficult to determine, as is the pass off of scattered photons from layer to layer. Nonetheless, the accuracy of the floor and ceiling shielding estimate is important as much of the cost of the total clinic shielding is driven by the construction costs related to the suspended lead. Consequently, three-dimensional Monte Carlo models for MCNP5^[3] were developed for the quiet and scanner rooms of a generic PET clinic.

The models are defined in the Moritz geometry editing code^[4] using parameters^[5] representing dimensions and shield thicknesses. Moritz propagates a change in one of these values throughout the model before it prepares an input file for MCNP. The models may be used to provide facility-specific shielding designs by simply modifying the dimensions of the rooms and concrete deck thickness to match those found in individual facility design plans.

In this work we use the models to calculate the attenuation provided by common thicknesses of concrete and layers of lead used for ceiling and floor shields. Both models assume a floor to ceiling distance of 4.27 m (14 feet).

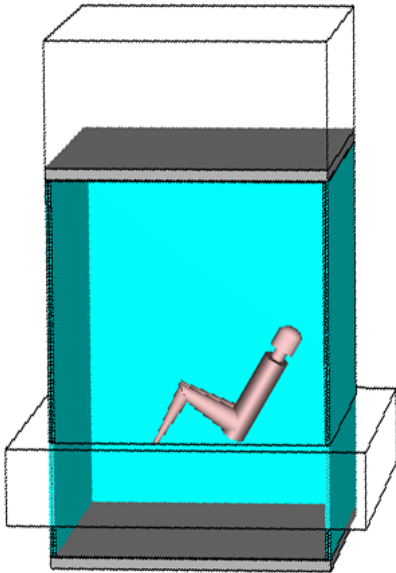


Fig. 1. The quiet room model.

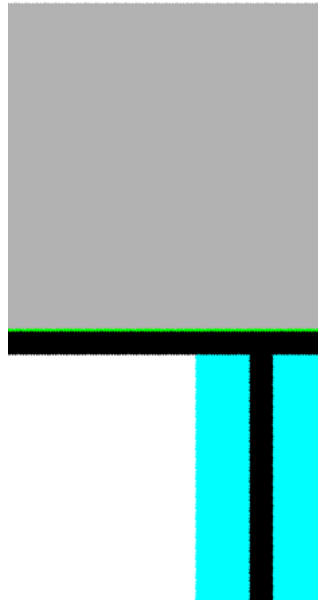


Fig. 2. Detail of wall and ceiling showing wallboard (blue), lead (black), steel decking (green), and concrete (grey).

Quiet Room

The quiet room model, shown in Fig. 1, consists of a male MIRD^[6] anthropomorphic model modified to a sitting posture^[7] inside a room. The inside room dimensions, taken from design plans for one clinic we evaluated, are 2.43 m (8 feet) along the human model axis, 2.13 m (7 feet) across, and 3.67 m (12 feet) high. The bottom of the human trunk is centered in the room approximately 0.67 m above the floor. A transformation applied to the room results in a reclining position with the vertical axis of the human model at 30° relative to the room vertical. (The human model was not transformed to facilitate source positioning.) . The walls consist of a 0.635 cm (1/4 inch) lead layer sandwiched between 1.59 cm (5/8 inch) layers of gypsum wallboard (blue in Fig. 2).

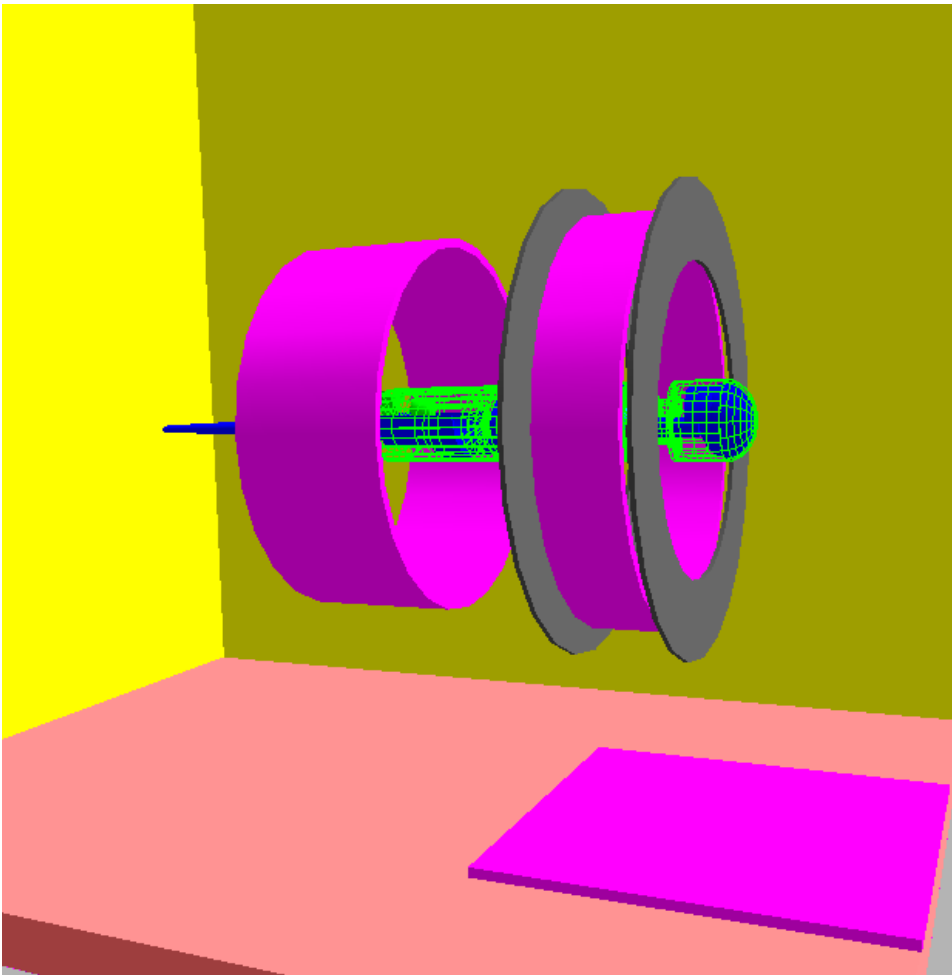


Fig. 3. The scanner room model.

The source consists of two 0.511 MeV photons per ¹⁸F disintegration with half of the 555 MBq (15 mCi) activity uniformly distributed throughout each of the brain and bladder. Self-attenuation of photons in the patient is correctly modeled in this manner. The Moritz code was used to plot the positions of a few hundred source points to verify that the source was confined to the brain and bladder.

Scanner Room

The scanner room model, shown in Fig. 3, is derived from common plans of scanner rooms in PET/CT facilities and uses a MIRD phantom placed supine in a combination PET/CT scanner. The model uses the same floor to ceiling height as the quiet room model and interior dimensions of 2.43 m (8 feet) x 3.05 m (10 feet). The PET/CT scanner was modeled based on figures provided by GE for their current PET and Multi-Slice CT unit, but may be extrapolated to all modern PET/CT units with multi-slice CTs. The model, shown in Fig. 3, consists of iron PET and CT rings with a thickness to match the attenuation of the actual rings. The base plates for the scanner and lead isolation rings between the PET and CT gantries were also modeled. The information for the PET/CT unit was provided by GE Healthcare^[8] based on their current designs. This model provides a realistic estimate of the attenuation provided by the PET/CT unit.

The source term assumes a patient load of 277 MBq (7.5 mCi) of ¹⁸FDG remains after the patient has rested in the quiet room for 45 minutes and then urinated. Thirty percent of the activity is located in the brain and the rest is distributed throughout the body. The correct source distribution was verified by plotting several hundred source points with the Moritz code.

MCNP Calculations

Since the source terms and the geometry for these models are complex, grids of tallies were used in air above and below the rooms to determine the position and value of maximum dose rate for the floors above and below. A dose response function was applied to the volume flux (F4) tallies. The tally volumes were ¼ m thick in the vertical direction centered 0.5 m in the upper rooms and 1.7 m above the floor of the room below. Additional tallies just above the floor and below the ceiling of the quiet and scanner rooms were taken to measure the variation of dose rates within the rooms. Numerous runs were made to provide a matrix of attenuation factors for common concrete deck (5.08, 10.16, 15.24, and 20.32 cm [2, 4, 6, and 8 inches]) and lead (0, 0.15875, 0.33175, and 0.635 cm [0, 1/16, 1/8, and ¼ inches]) thicknesses used to construct these shields. Importance splitting was used through the layers of the shields. Sufficient histories were run to ensure all relative errors were < 8% and the MCNP statistical tests were passed.

RESULTS

The tallies show that the largest dose rates are directly above and below the patient's head in the quiet room. For the scanner room, the high point on the floor above was also above the patient's head, but is shifted to the center of the phantom in the floor below the scanner due to added attenuation provided under the patient's head by the scanner base plate. The variation among the tallies the upper and lower rooms is small—no more than a factor of 4 for both the quiet and scanner room models and less than a factor of 2 in ½ of the cases. Fig. 4 shows a 3D view of the scanner room and the tallies in the upper and

lower rooms with the tallies color coded by dose rate in arbitrary units. Fig. 5 shows 2D views of the same tallies.

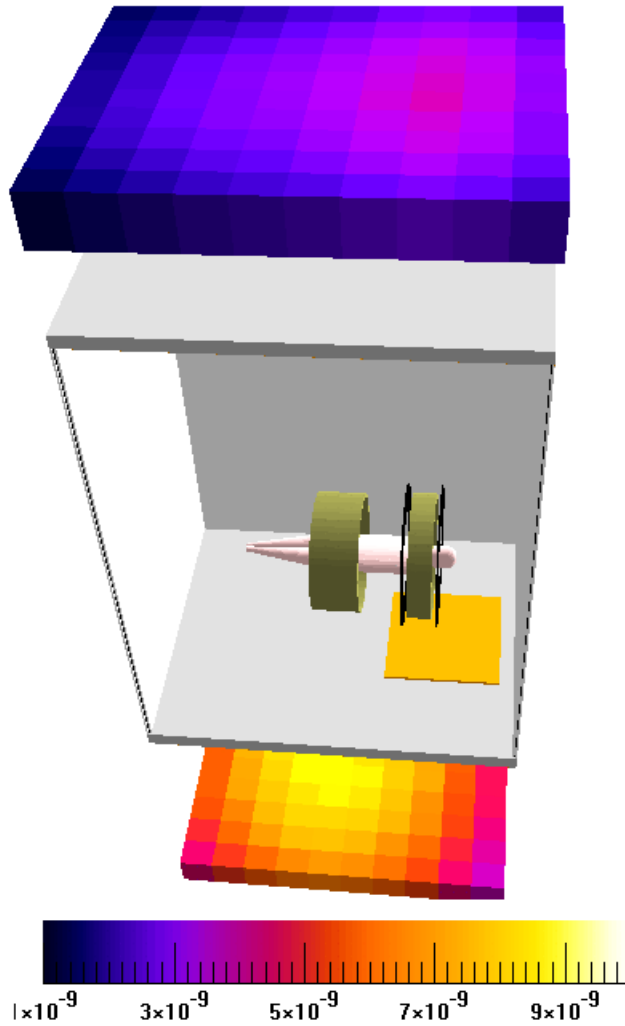


Fig. 4. 3D view of the tallies in the rooms above and below the scanner room colored coded by the dose rate in arbitrary units.

Attenuation Factors

We define the attenuation as the ratio of the dose rate from one region in a model with no floor or ceiling shielding to the rate from the same region in a shielded model. We consider two locations—the tally volumes in the upper and lower rooms. The attenuations were calculated for each of these regions. Because of the variation in dose rates in these regions, the attenuation depends on the specific tally or tallies chosen for the ratio. Two methods were considered. One uses the ratio of the largest dose rates in

each location. The other takes the average dose rates in each location. Neither method gives attenuation factors that were consistently higher or lower than the other method. Tables I through IV show the attenuation factors based on the average method. The columns are labeled by the lead thickness (in cm) and the rows by the concrete thickness (in cm). Any application of the factors should take note of the variation of the dose rate with position, the height at which the tallies were taken, and the floor to ceiling height assumed in the models.

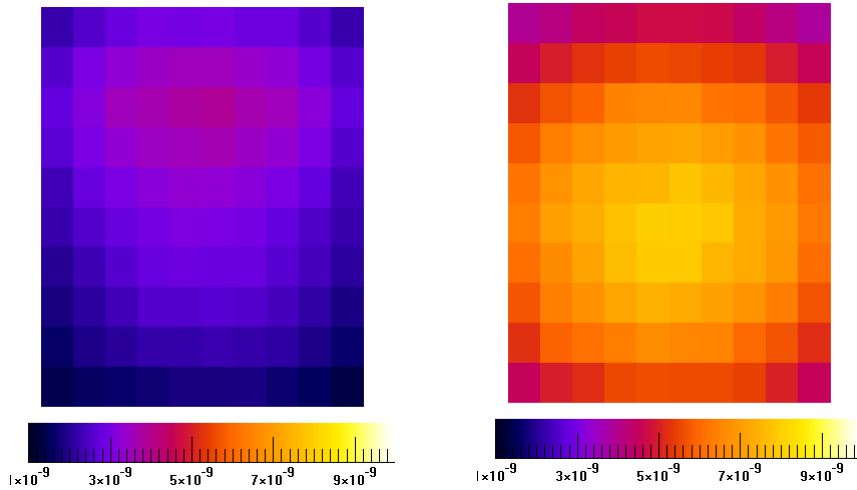


Fig. 5. 2D views of the tallies in the rooms above (left) and below (right) the scanner room colored by the dose rate in arbitrary units.

TABLE I. Attenuation Factors for Room Above Quiet Room.

Concrete/Lead	0	0.15875 (1/16")	0.33175 (1/8")	0.635 (1/4")
5.08 (2")	1.86	2.77	3.74	6.53
10.16 (4")	3.89	5.58	7.48	13.01
15.24 (6")	8.52	11.91	15.89	27.54
20.32 (8")	19.23	26.39	34.99	60.49

TABLE II. Attenuation Factors for Room Below Quiet Room.

Concrete/Lead	0	0.15875 (1/16")	0.33175 (1/8")	0.635 (1/4")
5.08 (2")	1.95	2.99	4.10	7.28
10.16 (4")	4.10	6.08	8.31	14.93
15.24 (6")	9.04	13.04	17.79	31.78
20.32 (8")	20.61	29.00	39.41	70.62

TABLE III. Attenuation Factors for Room Above Scanner Room.

Concrete/Lead	0	0.15875 (¹ / ₁₆ "	0.33175 (¹ / ₈ "	0.635 (¹ / ₄ "
5.08 (2")	1.82	2.73	3.70	6.44
10.16 (4")	3.80	5.45	7.34	12.77
15.24 (6")	8.28	11.55	15.48	26.81
20.32 (8")	18.64	25.57	34.05	58.81

TABLE IV. Attenuation Factors for Room Below Scanner Room.

Concrete/Lead	0	0.15875 (¹ / ₁₆ "	0.33175 (¹ / ₈ "	0.635 (¹ / ₄ "
5.08 (2")	1.75	2.57	3.47	5.99
10.16 (4")	3.52	5.05	6.81	11.89
15.24 (6")	7.62	10.71	14.39	25.15
20.32 (8")	17.21	23.82	31.97	55.75

Comparison with AAPM Values

The American Association of Physicists in Medicine (AAPM) has issued a guide for shielding in PET clinics^[9]. The guide includes a table of attenuation factors for various thicknesses of lead, concrete, and iron. Table V compares our results for concrete only shields to the AAPM results. Our results show more attenuation by factors between 1.5 and 1.7. The AAPM results are based on Monte Carlo calculations by one of the guide's authors (D. Simpkin) who assumed a 511 keV broad beam incident on the shields. In our models, the average energy of photons entering the shields is between 300 and 250 keV because of down scattering in the patient. The lower photon energies result in more attenuation by the shields.

TABLE V. Comparison of Attenuation Factors without Lead Layer.

Concrete Thickness

	Table I	AAPM	Tab. I/AAPM
5.08 (2")	1.75	1.27	1.47
10.16 (4")	3.52	2.50	1.56
15.24 (6")	7.62	5.00	1.70
20.32 (8")	17.21	11.11	1.73

Scanner Attenuation

Some shielding is provided to the areas above and below the scanner room by the double gantry of the scanner and the base plate. To investigate how much it contributes to the attenuation, we compared the tallies from the model of the scanner room with no floor and ceiling shielding and the scanner model present to the results from a model where the scanner gantries and base plate are replaced by air (but with the patient present). For the upper and lower rooms, the additional average attenuation factors are 1.6 and 2.3, respectively. The scanner model includes a large steel plate on the floor that contributes to the greater attenuation for the lower room.

CONCLUSIONS

We have run a number of Monte Carlo calculations for various combinations of lead and concrete shielding in the floor and ceiling of typical quiet and scanner rooms in a PET clinic. We have developed models in which the room dimensions and shielding thicknesses can easily be adjusted to match a specific configuration. Down scattering of the photon energy within the patient results in more attenuation through the shields than when assuming a 511 keV photon energy incident on the shield. The PET and CT rings contribute a factor of 2 to the total attenuation.

REFERENCES

1. A. CHILTON, R. FAW, J. SHULTIS, *Principles of Radiation Shielding*, Prentice-Hall, Englewood Cliffs, USA (1984).
2. D. K. TRUBY, et al., *Gamma-ray attenuation coefficients and buildup factors for engineering materials*, American Nuclear Society, LaGrange Park, IL, ANSI/ANS-6.4.3-1991 (1992).
3. J. F. BRIESMEISTER, Editor, *MCNP – A General Monte Carlo N-Particle Transport Code*, Los Alamos National Laboratory Report LA-13709-M, (2000).
4. K. A. VAN RIPER, “Interactive 3D Display of MCNP Geometry Models,” *Proceedings of the ANS International Meeting on Mathematical Methods for Nuclear Applications*, Salt Lake, UT, Sept. 10–13, (2001).
5. K. A. VAN RIPER, “Parameterized Combinatorial Geometry Modeling In Moritz,” *Proceedings of Mathematics and Computation, Supercomputing, Reactor Physics and Nuclear and Biological Applications*, Palais des Papes, Avignon, France, September 12-15, 2005, on CD-ROM, American Nuclear Society, LaGrange Park, IL (2005).
6. M. CRISTY, K. F. ECKERMAN, *Specific Absorbed Fractions of Energy at Various Ages from Internal Photon Sources. I. Methods*, Oak Ridge National Laboratory Report ORNL/TM-8381/VI (1987).
7. R. H. OLSHER, K. A. VAN RIPER, *Application of a Sitting MIRD Phantom for Effective Dose Calculations*, Proceedings of the ICRS-10/RPS 2004 Conference, 9–14 May 2004, Funchal, Portugal (Radiation Protection Dosimetry, in press) (2005).
8. J. WILLIAMS, Ph.D., GE Healthcare, private communication (2005).
9. M. T. MADSEN, J. A. ANDERSON, J. R. HALAMA, J. KLECK, D. J. SIMPKIN, J. R. VOTAW, R. E. WENDT III, L. E. WILLIAMS, and M. V. YESTER, *Draft AAPM Guide on PET and PET/CT Shielding Requirements*, AAPM (2004).